Available online at www.sciencedirect.com

ScienceDirect

Catalysis Today 133–135 (2008) 534–540

CATALYSIS TODAY

www.elsevier.com/locate/cattod

De–SO_x additives based on mixed oxides derived from Mg,Al-hydrotalcite-like compounds containing Fe, Cu, Co or Cr

Carla Maria Salerno Polato [a,1], Cristiane Assumpção Henriques [b,*], Alexandre Carlos Camacho Rodrigues [a,2], José Luiz Fontes Monteiro [a]

[a] NUCAT-COPPE/UFRJ, PO Box 68502, CEP 21945-970, Rio de Janeiro, Brazil
[b] IQ/UERJ, Rua São Francisco Xavier 524, CEP 20559-900, Rio de Janeiro, Brazil

Abstract

Mg,Al-hydrotalcite-like compounds (HTLCs) with an $M^{3+}/(M^{2+} + M^{3+})$ molar ratio equal to 0.25 in which Mg or Al were partially replaced by Cu, Co, Cr or Fe were prepared and used as precursors for different mixed oxides (MO): Cu–MO, Co–MO, Cr–MO or Fe–MO. These materials were evaluated for SO_x removal under conditions similar to those found in the fluid catalytic cracking (FCC) regenerator. The following order of catalytic activity for SO_x uptake was observed: Cu–MO > Co–MO > Fe–MO > Cr–MO. The regeneration of the sulfated additives was also studied and the results showed that the composition of the reductive stream influenced the regeneration profiles, the total quantity of sulfur released, and the reduction products distribution, in a specific way for each sample. These results could be related to the nature of the reducing agent and to the fact that the thermal stability and the reducibility of the sulfates are significantly affected by the metal with redox properties present in the additive.

Keywords: SO_x emission control; Sulfur-transfer catalysts; FCC unit; Mg,Al-mixed oxides; Fe; Cu; Co; Cr

1. Introduction

The fluid catalytic cracking (FCC) is a refining process that converts gas oil and other heavy feedstocks into lighter, more valuable products such as gasoline and distillate fuel. The FCC unit (FCCU) consists basically of a reactor and a regenerator. The cracking of the heavy hydrocarbon molecules is carried out in the riser section of the reactor, while the oxidation of the coke deposited on the catalyst during cracking in the riser takes place in the regenerator [1]. If a sulfur containing feedstock is fed into a FCC unit without pretreatment, 45–55% of the total sulfur presented is released as H_2S and 35–45% stays in the liquid products as sulfur compounds. About 5% of the total sulfur fed is left on the catalyst as part of the coke and is converted into sulfur oxides (10% SO_3 and 90% SO_2) that are released to the atmosphere during coke burn-off in the regenerator [1–5]. Since these gases are among the major atmospheric pollutants and are acid rain precursors, their emission is increasingly restricted by environmental legislation.

Considering the reduction of SO_x emissions in the FCCU, the least costly strategy is the addition of SO_x transfer additives to the FCC catalyst. Those additives adsorb SO_x and so transfer sulfur back into the riser where it is released as H_2S, which is removed in the usual way (Claus process). This technique is very practical since the use of additives requires almost no capital investment, except for the cost of an additive loading system and the availability of a Claus plant. Three steps determine the performance of a SO_x transfer catalyst: (1) the oxidation of SO_2 to SO_3 under the FCC regenerator conditions (typically at 680–730 °C); (2) the trapping of SO_3 on the catalyst in the form of sulfates and (3) the reduction of sulfates to release sulfur as H_2S in the FCC riser (typically at 520–530 °C) [1,2,5–11].

As to the composition of the transfer catalysts, compounds of intermediate basicities such as Mg,Al-mixed oxides and/or

---

* Corresponding author. Fax: +55 21 25877172.
E-mail address: cah@uerj.br (C.A. Henriques).

[1] Present address: INPI, Instituto Nacional de Propriedade Industrial, Rio de Janeiro, Brazil.

[2] Present address: ANP, Agência Nacional de Petróleo, Gás Natural e Biocombustíveis, Rio de Janeiro, Brazil.

0920-5861/$ – see front matter © 2007 Elsevier B.V. All rights reserved.
doi:10.1016/j.cattod.2007.12.046

spinels ($MgAl_2O_4$) derived from hydrotalcite-like compounds are among the most promising. These species present a large capacity of SO_3 uptake, forming sulfates that can be reduced in the reductive atmosphere of the riser [2,3,5,7–11]. Since the SO_3 content in the regenerator is relatively low, the addition of promoters with redox properties as co-catalysts is necessary. These compounds should catalyze not only the oxidation of SO_2 to SO_3 in the regenerator but also the recovery of the basic oxides in the riser. Literature reports the incorporation of different metallic oxides, such as those of Ce, Cu, Co, V, Cr and Fe, to hydrotalcite-like compounds (HTLC), either by impregnation or coprecipitation, as the best way to generate the mixed oxides/spinels solid solutions with both basic and redox properties needed for good performance on De–SO_x process [1–7,10,12,13]. However, comparing the results reported by different authors is often not feasible due to the diversity of both the experimental conditions explored and the type of technique used to follow the various steps related to the process. Another aspect not usually explored is the nature of the reductive agent responsible for the regeneration of the sulfated additive (hydrocarbons or H_2, for instance).

In the present work, Mg,Al-mixed oxides with $M^{3+}/(M^{2+} + M^{3+})$ molar ratio equal to 0.25, derived from Mg,Al-HTLCs containing copper, iron, chromium or cobalt, were comparatively evaluated as SO_x transfer catalysts. A stream containing SO_2 and O_2 was used in the oxidative adsorption step, under conditions similar to that found in the regenerator of FCC units. For the catalyst regeneration step, two distinct reductive streams were compared: 30%H_2/He and 30%C_3H_8/He.

2. Experimental

2.1. Synthesis of the hydrotalcite-like precursors

Hydrotalcite-like compounds were prepared with an $(M^{3+})/(M^{2+} + M^{3+})$ molar ratio of 0.25, by coprecipitating, at room temperature, an aqueous solution of the metallic cations (solution A) with a highly basic carbonate solution (solution B), under vigorous stirring. The synthesis gels so produced had the following compositions:

$$2.25Mg(NO_3)_2 : 0.75Al(NO_3)_3 : 2Na_2CO_3 : 6.75NaOH$$

or

$$0.375M(NO_3)_2 : 1.875Mg(NO_3)_2 : 0.75Al(NO_3)_3 : 2Na_2CO_3 : 6.75NaOH$$

or

$$2.25Mg(NO_3)_2 : 0.375T(NO_3)_3 : 0.375Al(NO_3)_3 : 2Na_2CO_3 : 6.75NaOH$$

where M refers to the divalent cation (Co^{2+} or Cu^{2+}) that partially replaces Mg^{2+} cations and T refers to trivalent cation (Fe^{3+} or Cr^{3+}) that partially replaces Al^{3+} cations. The molar ratios M/Mg (0.20) and T/Al (1.0) were selected in order to reach a transition metal content close to 11% (molar base) [7]. The gel was aged under constant pH (13) for 18 h at 60 °C (exception for the Cr-containing sample, which was aged for 7 days). The solid obtained was then filtered, washed with distilled water (90 °C) until pH 7 and dried at 80 °C overnight. The synthesized samples were named HT (Mg,Al-hydrotalcite), MHT or THT, where M or T is the cation that partially replaces Mg or Al, respectively. The mixed oxides were obtained by calcining HTLCs precursors under dry air from room temperature to 750 °C, at a 10 °C/min heating rate, and keeping at this temperature for 2 h. The calcined samples were named MO, M–MO or T–MO (M and T defined as above).

2.2. Physico-chemical characterization

The chemical composition of the synthesized samples was determined by X-ray fluorescence using a Rigaku Rix 3100 spectrometer. In order to identify the crystalline phases formed on both the HTLCs and the mixed oxides, X-ray powder diffractograms were recorded in a Rigaku X-ray Diffractometer equipped with a graphite monochromator using Cu Kα, 40 kV and 40 mA, in the range 2θ from 10° to 80°. The software UnitCell [14] was employed for structural refinement aiming at calculating the lattice parameters, a and c. The textural characteristics, such as specific surface area (BET) and pore volume (BJH), were determined by N_2 adsorption–desorption at −196 °C in a Micromeritics ASAP 2000. The samples were previously outgassed at 200 °C overnight.

2.3. Chemical reaction

During the SO_2 pick-up reaction, a stream of 175 mL/min with 1630 ppm of SO_2, 1.6% (v/v) O_2 and He balance was passed over the catalyst in a fixed bed quartz micro-reactor at 720 °C. The adsorption cycle was finished after a time on stream of 4 h. For catalyst regeneration, the system was flushed with He and the sample was cooled down to 530 °C. Then, He was shut off and the catalyst was reduced in a stream of 130 mL/min of H_2 (30%)/He (70%) or C_3H_8 (30%)/He (70%), at 530 °C, for 30 min. After that, the temperature was ramped to 800 °C at 10 °C/min, under the same atmosphere. The evolution of the products, in both steps, was followed by on-line mass spectrometry using a Balzers quadrupole spectrometer (Model PRISMA-QMS 200). The presence of hydrogen ($m/z = 2$), water ($m/z = 18$), oxygen ($m/z = 16$ and 32), H_2S ($m/z = 33$ and 34), SO_2 ($m/z = 48$ and 64) and carbon dioxide ($m/z = 12$, 28 and 44) in the outflowing gases was monitored. Quantitative analyses were based on components peak areas and their fragmentation patterns, with adequate use of calibration standards and numeric deconvolution.

3. Results and discussion

3.1. Physico-chemical characterization

The X-ray diffractograms of the as-synthesized HTLC samples are shown in Fig. 1. Samples HT, Co–HT, Fe–HT and Cr–HT show the characteristic pattern of pure hydrotalcite in

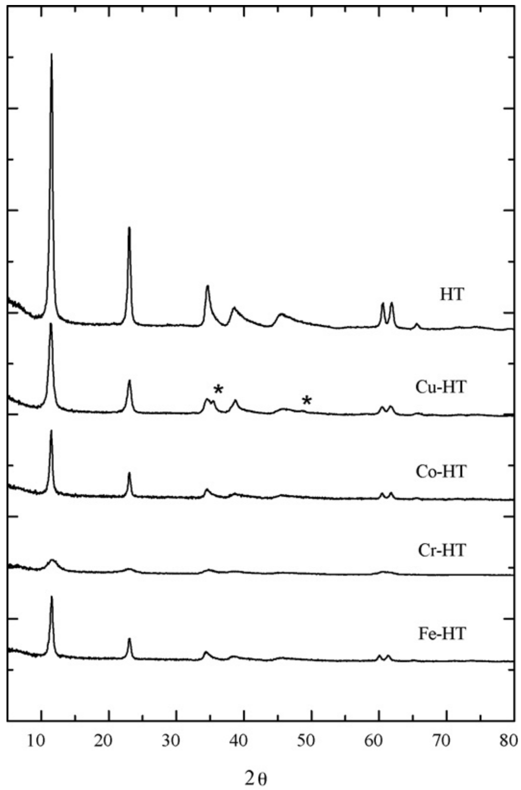

Fig. 1. X-ray diffraction patterns of the as-synthesized HTLCs precursors. (*) CuO–tenorite.

carbonate form, suggesting the complete incorporation of the transition metals into the crystalline structure, whereas for sample Cu–HT, besides the hydrotalcite peaks, diffraction lines at 2θ equal to 35.45° and 48.75°, corresponding to CuO–tenorite (*) [15] were observed. The chromium-containing sample (Cr–HT) showed a very low crystallinity, even after a large aging time (7 days, instead of 18 h), suggesting a very low crystallization kinetics when compared to the others.

The lattice parameters, *a* and *c*, typical of hydrotalcite structures with rombohedral 3R symmetry were calculated for all samples from the peaks associated to planes (0 0 3), (0 0 6), (1 1 0) and (1 1 3) and are shown in Table 1 along with the ionic radius of the cations present in each HTLC structure. Comparing the values of parameter *a*, which is a function of the cation–cation distance in the hydroxide layers [16], it can be observed that their differences are compatible with those existent between Mg^{2+} or Al^{3+} ionic radius and those of the transition metal di- or trivalent cations. This is an evidence that these transition metal cations have isomorphously replaced Mg^{2+} or Al^{3+} in the HTLC structure. Parameter *c*, which is related to the layer thickness (brucite-like sheet plus an interlayer), depends upon several factors such as the amount of interlayer water, the size of the interlayer anion and of the M^{2+}–M^{3+} cations, and the strength of the electrostatic attractive forces between the layer and the interlayer [16,17]. The results shown in Table 1 must probably reflect the influence of these various factors.

Table 2
Chemical composition and textural characteristics of HTLCs

Sample	Molar composition		S_{BET} (m^2/g)	V_{meso} (cm^3/g)[a]
	Gel	Sample		
Mg/Al	6.0/2.0	6.06/1.94	71	0.378
Cu/Mg/Al	1.0/5.0/2.0	0.81/5.25/1.94	76	0.413
Co/Mg/Al	1.0/5.0/2.0	0.95/5.11/1.94	69	0.489
Cr/Mg/Al	1.0/6.0/1.0	0.88/6.12/1.00	170	0.190
Fe/Mg/Al	1.0/6.0/1.0	0.91/6.12/0.97	71	0.490

[a] Calculated by BJH method.

Table 2 shows the physico-chemical characteristics of the as-synthesized HTLCs. As can be observed, their chemical composition was quite similar to that of the corresponding synthesis gel, indicating that the metallic cations were incorporated at the expected levels. As to the textural characteristics, Table 2 show that, except for sample Cr–HT, the partial replacement of Mg or Al by Cu, Co or Fe did not have a significant effect on BET specific surface area when compared to those of pure Mg,Al-hydrotalcite (sample HT), but increases mesoporous volume. On the other hand, the textural properties of sample Cr–HT could be reflecting its smallest crystallite size associated to its lowest crystallization rate.

XRD diffractograms (Fig. 2) indicate that, upon calcination at 750 °C, the layered structure of HTLCs collapsed, forming a poorly crystallized Mg(Al)O with a periclase-type structure ($2\theta = 35.7°$, 43.40° and 62.90°) [15] in which the oxides of the transition metals were dispersed. Except for Cr–MO sample, the formation of spinel-type phase was not detected for the samples calcined at 750 °C. For sample Cu–MO, besides the Mg(Cu, Al)O-periclase phase, characteristic peaks associated to the CuO–tenorite phase were also observed. This phase was already present in the precursor material and became more evident after thermal treatment at 750 °C. This result differs from those of Chmielarz et al. [18] which studied a Cu,Mg,Al-hydrotalcite with similar composition and detected the segregation of a CuO-phase only for the sample cooled down

Table 1
Lattice parameters of the as-synthesized HTLCs

Sample	*a*	*c*	Ionic radius (Å) [21]
HT25	3.0536	23.1392	$Mg^{2+} = 0.65$ $Al^{3+} = 0.50$
Cu–HT25	3.0602	23.3020	$Cu^{2+} = 0.69$
Co–HT25	3.0596	23.2677	$Co^{2+} = 0.74$
Fe–HT25	3.0791	23.0999	$Fe^{3+} = 0.64$
Cr–HT25	–	–	$Cr^{3+} = 0.69$

Table 3
Textural characteristics of mixed oxides

Sample	S_{BET} (m^2/g)	V_{meso} (cm^3/g)[a]
MO25	213	0.747
Cu–MO25	114	0.495
Co–MO25	179	0.656
Cr–MO25	118	0.365
Fe–MO25	140	0.617

[a] Calculated by BJH method.

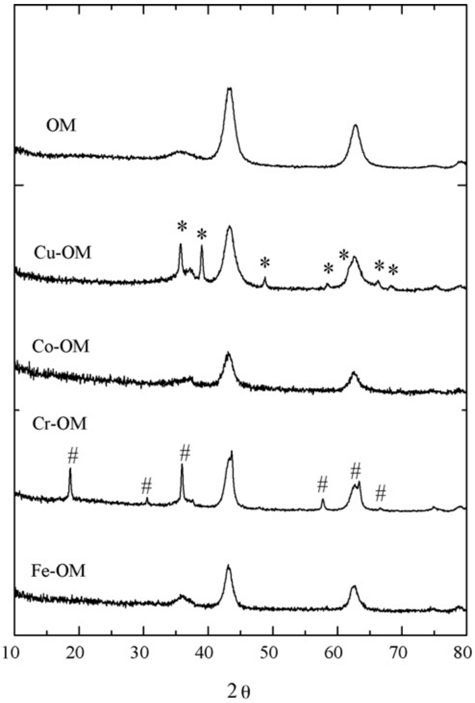

Fig. 2. X-ray diffraction patterns of the mixed oxides derived from HTLCs after calcination at 750 °C. (*) CuO–tenorite; (#) $MgCr_2O_4$-spinel.

at room temperature after calcination at 1000 °C. For the chromium-containing sample (Cr–MO), a magnesiumcromite phase ($MgCr_2O_4$) [15], with a spinel-type structure, was identified along with the periclase phase (Mg(Cr, Al)O). On the other hand, X-ray diffratograms of samples Co–MO and Fe–MO indicate that cobalt and iron oxides are well dispersed in the Mg(Al)O phase.

Inspection of the N_2 adsorption/desorption results indicated that all samples presented IUPAC type IV isotherms, confirming that the thermal decomposition of the hydrotalcite-like samples at 750 °C produced mesoporous mixed oxides. Their main textural characteristics are shown in (Table 3). Except for sample Cr–MO, the collapse of the layered structure upon thermal treatment increased both the BET specific surface area and the mesoporous volume. The increase of the mesoporous volume seems to be associated to descarboxylation and dehydroxylation through a cratering mechanism which starts around 280 °C and leads to a destruction of the layered structure with the formation of new pores. As reported by Chmielarz et al. [18], the transition metal containing HTLCs presented lower BET specific surface areas the related Mg,Al sample. For sample Cr–HT, the thermal treatment at 750 °C increased its mesoporous volume but reduced its BET specific surface area. These changes in textural characteristics could be associated to the formation of pores with diameter in the range 80–200 Å from the collapse of the 20–60 Å mesopores present on the parent Cr–HT. This suggests that this sample consists of small unstable crystals. For the Cu-containing sample, the CuO phase could be blocking the pores so explaining the lower textural modification observed for this sample.

Table 4
SO_x pick-up efficiency (reaction conditions: T = 720 °C, 1 atm, 1630 ppm SO_2, 1.6% (v/v) O_2 and He balance, for 4 h TOS)

Sample	SO_2 uptake (μmol SO_2/g)	Theoretical (μmol SO_2/g)[a]	SO_x pick-up efficiency (%)
OM25	400	17660	2.3
Cu–OM25	14928	13695	109
Co–OM25	12661	13589	93
Cr–OM25	8263	16789	49
Fe–OM25	8420	16596	51

[a] Calculation based on the assumption that only Mg atoms are available for sulfur pick-up.

3.2. Catalytic tests

The performance of the catalysts for SO_2 uptake is compared in Table 4. The results show the following order of SO_2 pick-up capacity: Cu–MO > Co–MO > Fe–MO > Cr–MO ≫ MO. The theoretical sulfur uptake levels were calculated based on the assumption that only Mg atoms in the mixed oxides are available for sulfur pick-up, forming sulfates [10].

For all samples it was possible to observe that the maximum rate of SO_x pick-up took place in the first 5 min of reaction (Fig. 3), which is extremely interesting since the contact time inside the FCC regenerator is about 5 or 10 min, depending on its operation mode (partial or total combustion, respectively). However, although sample Co–MO was the second most active sample for SO_2 removal, it exhibited a different behavior, as can be observed in Fig. 3. For this catalyst, SO_2 oxidative adsorption takes place in two specific steps, the second (after about 2 h on stream) being the most important. Since the maximum reaction time on the regenerator of FCC units is 10 min, this sample does not show promising results for SO_x removal at short reaction times.

The regeneration of the sulfated catalysts was studied under two different reductive atmospheres: 30%H_2/He or 30%C_3H_8/He. It was observed that the composition of the reductive stream influenced the catalyst regeneration profile, the total

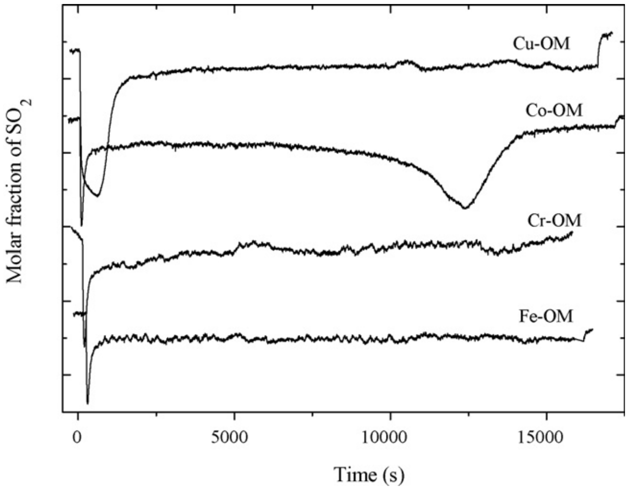

Fig. 3. SO_2 adsorption profile (T = 720 °C, 1630 ppm SO_2, 1.6% (v/v) O_2 and He balance).

Table 5
Effect of reductive stream composition on additive regeneration after sulfation under 1630 ppm SO_2, 1,6% de O_2 and He balance

Sample	Cu–OM25		Co–OM25		Cr–OM25		Fe–OM25	
Reductive stream[a]	1	2	1	2	1	2	1	2
SO_2 pick-up (μmol/g)	14928	13795	12661	12611	8263	10452	8420	6789
Regeneration (%)	74	29	79	69	77	15	84	66
Sulfur release (%)								
As SO_2	6	9	14	12	10	5	21	2
As H_2S	68	20	65	57	67	10	63	64

[a] (1) 30%H_2/He or (2) 30%C_3H_8/He.

amount of sulfur released, and the distribution of the reduction products, in a different way for each one of the catalysts, as shown in Table 5 and in Figs. 4–11. These results suggest that the nature of the metal with redox properties influences both thermal stability and sulfate reducibility, since it plays a role not only in the sulfation step but also in the regeneration of the sulfated catalyst, as proposed by Wang et al. [4] for $MgAl_{2-x}Fe_xO_4$ catalyst. According to these authors, oxygen vacancies associated to the transition metal (M) are the sites for oxygen adsorption and sulfate ion is formed from the reaction between these adsorbed oxygen species (O^-) and sulfite-like species (SO_3^-). As to the reduction process, hydrogen probably first attacks S–O–M bond and captures an oxygen ion. This breaks of the bond between ions M and S, with the formation of an oxygen vacancy and reduced metal species. Moreover, the redistribution of electron density around the sulfur ion group associated to its instability favors the weakening of the MgO–SO_2 bond. The maintenance of the reduction process with hydrogen would then produce a large quantity of H_2S.

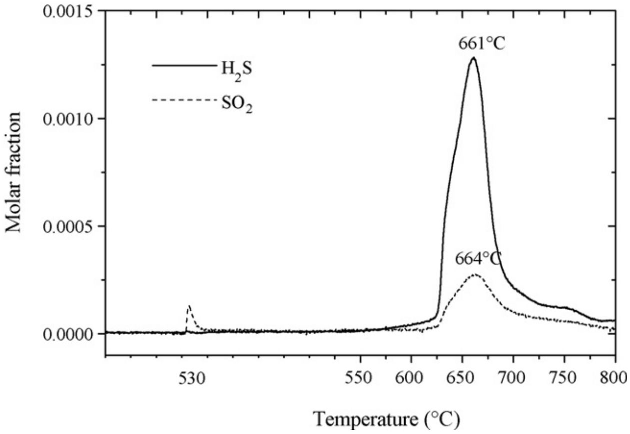

Fig. 4. Reduction profile for the sulfated Cu–MO (30%H_2/He for 30 min, at 530 °C. After that, the temperature was ramped to 800 °C at 10 °C/min).

Furthermore, the reduction of the sulfated species is also dependent on the reductive stream. According to Kim and Juskelis [6], the reduction of the sulfate species is a consecutive sequence of events having S^{4+} species as intermediates. The metallic oxide with redox properties plays a role not only in the reduction of sulfur species but also in the providing of active hydrogen, as illustrated below.

$$HC{-}H(\mathrm{or}H_2) + M^{x+} + e \leftrightarrows (HC{-}H)^+ + [H^-] + M^{(x-1)+} \tag{1}$$

$$SO_3 + 2M^{(x-1)+} \leftrightarrows [SO_3{}^{2-}] + 2M^{x+} \tag{2}$$

$$[SO_3{}^{2-}] \leftrightarrows SO_2 + O^{2-} \tag{3}$$

$$SO_2 + O^{2-} + 8H \leftrightarrows H_2S + 3H_2O + 2e \tag{4}$$

$$(HC{-}8H)^{8+} + 8e \leftrightarrows (HC{-}8H) \tag{5}$$

where HC = hydrocarbon.

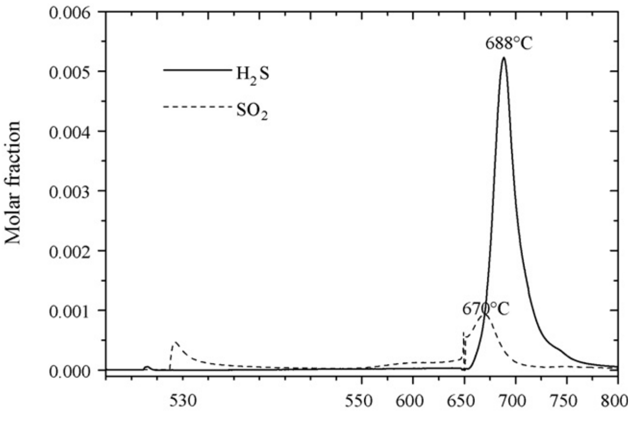

Fig. 5. Reduction profile for the sulfated Cu–MO (30%C_3H_8/He for 30 min, at 530 °C. After that, the temperature was ramped to 800 °C at 10 °C/min).

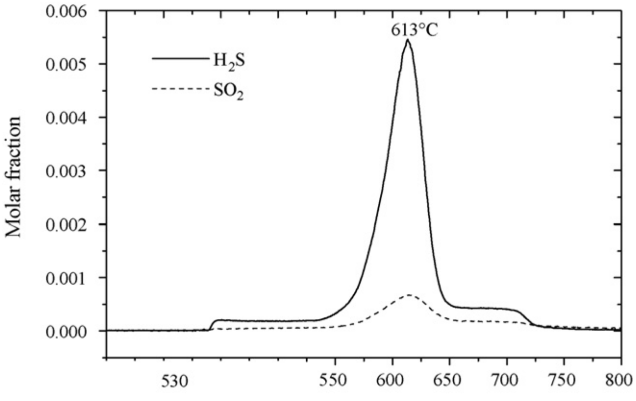

Fig. 6. Reduction profile for the sulfated Co–MO (30%H_2/He for 30 min, at 530 °C. After that, the temperature was ramped to 800 °C at 10 °C/min).

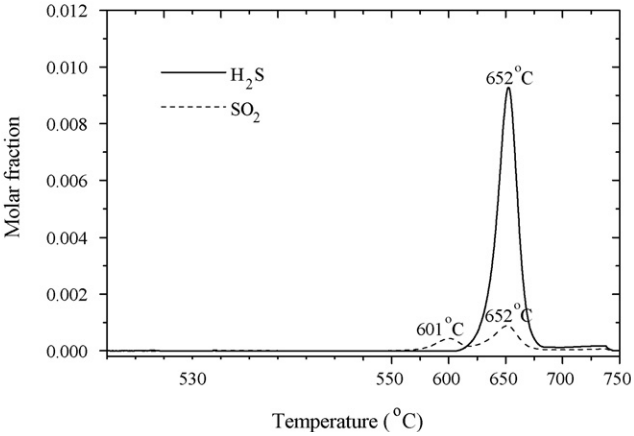

Fig. 7. Reduction profile for the sulfated Co–MO (30%C_3H_8/He for 30 min, at 530 °C. After that, the temperature was ramped to 800 °C at 10 °C/min).

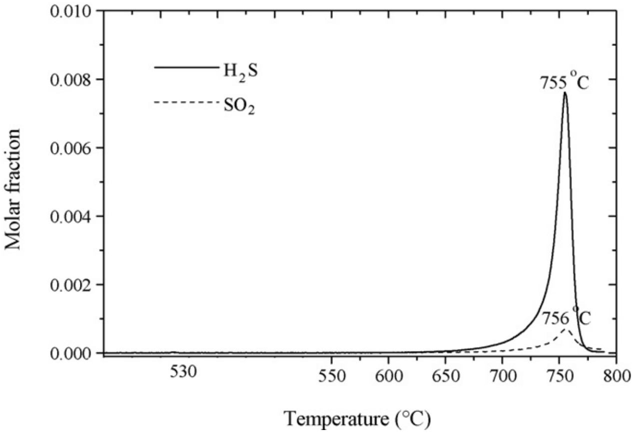

Fig. 10. Reduction profile for the sulfated Cr–MO (30%H_2/He for 30 min, at 530 °C. After that, the temperature was ramped to 800 °C at 10 °C/min).

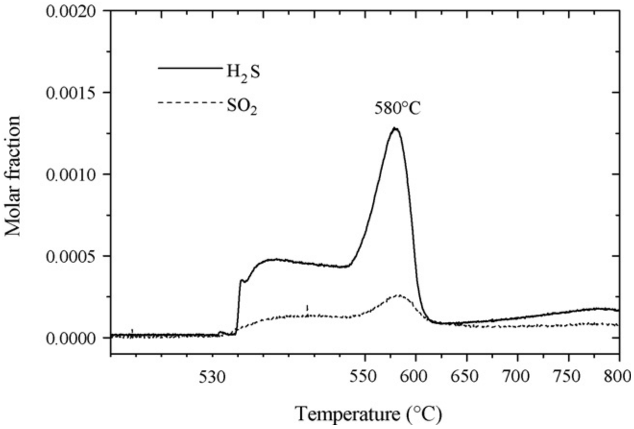

Fig. 8. Reduction profile for the sulfated Fe–MO (30%H_2/He for 30 min, at 530 °C. After that, the temperature was ramped to 800 °C at 10 °C/min).

For all the studied samples, in the presence of H_2 as reducing agent, the results shown in Table 5 indicated a regeneration level of the sulfated catalysts in the range 74–84%. The replacement of C_3H_8 for H_2 decreased the catalysts regeneration. This effect was slightly important for sample Co–MO but very significant for samples Cu–MO and mainly Cr–MO.

For sample Cu–MO, in the presence of H_2, H_2S was the main product from sulfate reduction, although a simultaneous evolution of SO_2 was also observed. Inspection of the reduction profiles (Fig. 4) shows that the onset temperature for H_2S release was about 580 °C, higher than that typical of an FCCU riser. With C_3H_8 as reducing agent, the relative amount of SO_2 released was much higher than in the presence of H_2. Fig. 5 shows that the H_2S release slightly shifts to higher temperatures and that in the presence of propane as reducing agent it was preceded by SO_2 evolution.

For the Co-containing sample (Co–MO), under H_2/He atmosphere, the onset temperature for H_2S release was similar to that of the riser of an FCCU (530 °C), with maximum at 613 °C. As observed for sample Cu–OM, the release of SO_2 was simultaneous to that of H_2S (Fig. 6). When propane was used as the reducing agent, the relative amount of H_2S and SO_2 released was similar to that under H_2. As to the reduction profiles, Fig. 7 shows that H_2S release shifted to higher temperatures (maximum at 652 °C) and that SO_2 was released in two clearly different temperatures, reinforcing the claim that

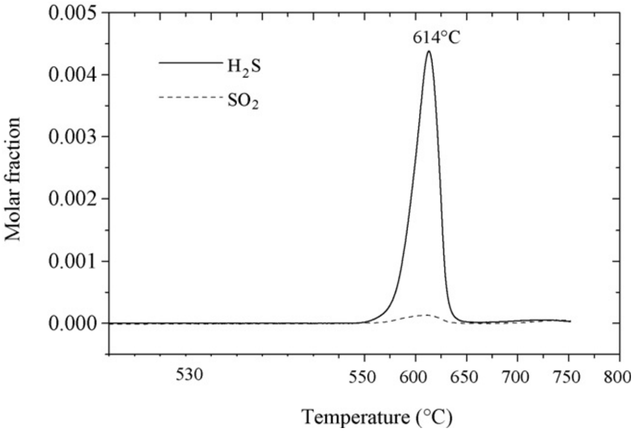

Fig. 9. Reduction profile for the sulfated Fe–MO (30%C_3H_8/He for 30 min, at 530 °C. After that, the temperature was ramped to 800 °C at 10 °C/min).

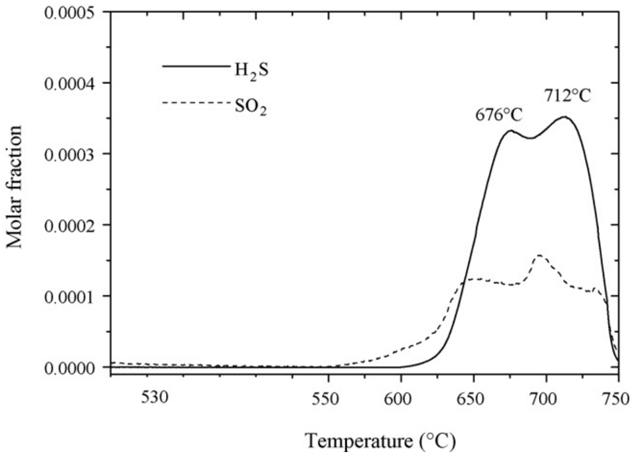

Fig. 11. Reduction profile for the sulfated Cr–MO (30%C_3H_8/He for 30 min, at 530 °C. After that, the temperature was ramped to 800 °C at 10 °C/min).

two types of sulfate species are involved [19]. These results agree with the reaction scheme proposed by Kim and Juskelis [6], according to which S^{4+} species are intermediates of the reduction of sulfate species (S^{6+}) to H_2S. However, they do not support the results observed by the same authors, in which the onset temperature for H_2S release was higher with H_2 as the reducing agent than with propane.

Regarding sample Fe–MO, Fig. 8 shows that, under H_2/He reducing atmosphere, the onset temperature for both H_2S and SO_2 was 530 °C, an interesting result considering the temperature of an FCCU riser. H_2S and SO_2 were simultaneously released and the presence of two distinct peaks at 530 and 580 °C could be observed. These results should be attributed to the existence of different sulfate species [19] or to a partial reduction of iron(III) species. As shown by Rodrigues et al. [20], the termoprogrammed reduction profile of sample Fe–MO showed two peaks, at 527 and 700 °C, being the first attributed to Fe(III) to Fe(II) reduction, possibly through Fe_3O_4, and the second related to the reduction of Fe(II) to metallic iron (9).

$$Fe_2O_3 \rightarrow Fe_3O_4 \rightarrow FeO \rightarrow Fe^\circ \qquad (6)$$

Inspection of Fig. 9 indicates that, in the presence of C_3H_8/He as reductive stream, H_2S and SO_2 evolution shifted to higher temperatures (T_{max} shifts from 580 to 614 °C). Both species were simultaneously evolved and no evidence of the existence of different sulfate species was observed. Furthermore, a remarkable reduction on the relative amount of SO_2 released was also observed, the reaction product being essentially H_2S.

As can be seen in Figs. 10 and 11, the highest temperatures for the reduction of the sulfated catalyst were observed for sample Cr–MO, regardless of the reducing agent employed. Differently from that observed for the other catalysts, release temperatures for H_2S and SO_2 were higher under H_2 than in the presence of propane. The reduction profiles were also significantly affected by the nature of the reducing agent, suggesting that the corresponding sulfate species presented different reactivities toward hydrogen or propane. In addition, the relative amount of sulfur released as SO_2 was the highest among the catalysts studied.

4. Conclusion

Mg,Al-mixed oxides derived from hydrotalcite-like compounds in which Mg or Al were partially replaced by a transition metal with redox properties were tested as SO_x transfer catalysts. They were more active for SO_x pick-up than the Mg,Al-mixed oxide (MO), confirming that the presence of a component with redox properties is essential for the use of these materials as additives to FCC catalysts aiming at removing SO_x formed in the FCCU regenerator. The following order of SO_x uptake efficiency was observed for the studied additives: Cu–MO > Co–MO > Fe–MO > Cr–MO ≫ MO.

The study of the influence of the composition of the reductive stream on catalytic performance indicated that propane was a less efficient reductive agent than hydrogen, as evidenced by the lower regeneration levels and by the higher temperatures for sulfur release. It was also observed that, under propane, H_2S release profiles were shifted to higher temperatures, except for the Cr-containing sample, which showed a different behavior when compared to the other samples. The observed results suggest that sulfate species reduction is strongly influenced either by the transition metal nature or by the reductive agent.

Acknowledgements

The authors thank CAPES (Carla Maria Salerno Polato D.Sc. scholarship). C.A. Henriques would like to thank PROCIENCIA Program of Universidade do Estado do Rio de Janeiro for the financial support.

References

[1] W.C. Cheng, G. Kim, A.W. Peters, X. Zhao, K. Rajagopalan, Catal. Rev. Sci. Eng. 40 (1998) 39.

[2] A. Corma, A.E. Palomares, F. Rey, Appl. Catal. B 4 (1994) 29.

[3] A. Corma, A.E. Palomares, F. Rey, F. Márques, J. Catal. 170 (1997) 140.

[4] J.A. Wang, Z.L. Zhu, C.L. Li, J. Mol. Catal. A 139 (1999) 31.

[5] A.A. Bhattacharyya, G. Woltermann, J.S. Yoo, J.A. Karch, W.E. Cormier, Ind. Eng. Chem. Res. 27 (1988) 1356.

[6] G. Kim, M.V. Juskelis, Study Surf. Sci. Catal. 101 (1996) 137.

[7] A.E. Palomares, J.M. Lópes-Nieto, F.J. Lázaro, A. Lópes, A. Corma, Appl. Catal. B 20 (1999) 257.

[8] J.A. Wang, C. Li, Appl. Surf. Sci. 161 (2000) 406.

[9] J.A. Wang, L.F. Chen, R. Ballesteros, A. Montoya, J.M. Dominguez, J. Mol. Catal. A 194 (2003) 181.

[10] C.M.S. Polato, C.A. Henriques, A. Alcover Neto, J.L.F. Monteiro, J. Mol. Catal. A 241 (2005) 184.

[11] J.S. Yoo, A.A. Bhattacharyya, C.A. Radlowski, Ind. Eng. Chem. Res. 30 (1991) 1444.

[12] A.J. Garcia, R. Cuevas, L.F. Pedroza, A.A. Vargas, M.C. Salcedo, B. Mar, J. Ramirez, Book of Abstracts 18th North American Catalysis Society Meeting, Cancun, Mexico, May, (2003), p. 233.

[13] J.S. Yoo, A.A. Bhattacharyya, C.A. Radlowski, J.A. Karch, Appl. Catal. B 1 (1992) 169.

[14] T.J.B. Holland, S.A.T. Redfern, Mineralog. Mag. 61 (1997) 65.

[15] ICDD PDF-2 Database (Release 1998)-International Centre for Diffraction Data (ICDD). 12 Campus Boulevard Newton Square, Pennsylvania 19073-3273, USA.

[16] I. Pausch, H.H. Lohse, K. Schurmann, R. Almann, Clays Clay Min. 34 (1086) 507.

[17] S. Velu, N. Shah, T.M. Jyothi, S. Sivasanker, Microporous Mesoporous Mater. 33 (1999) 61.

[18] L. Chmielarz, P. Kustrowski, A. Rafalska-Lasocha, R. Dziembaj, Thermochim. Acta 395 (2003) 225.

[19] A. Trovarelli, C. Leitenburg, M. Borao, G. Dolcetti, Catal. Today 50 (1999) 353.

[20] A.C.C. Rodrigues, C.A. Henriques, R.E. Roncolatto, J.L.F. Monteiro, in: Proceedings of the 12th Brazilian Congress on Catalysis, Angra dos Reis, vol. 1, Brazil, September, (2003), p. 290.

[21] F. Cavani, F. Triffiró, A. Vaccari, Catal. Today 11 (1991) 173.